HEWLETT-PACKARD JOURNAL
TECHNICAL INFORMATION FROM THE -hp- LABORATORIES
CORPORATE OFFICES • 1501 PAGE MILL ROAD • PALO ALTO, CALIFORNIA 94304 • VOL. 16 NO. 7, MARCH 1965

The Linear Quartz Thermometer— a New Tool for Measuring Absolute and Difference Temperatures

A linear-temperature-coefficient quartz resonator has been developed, leading to a fast, wide-range thermometer with a resolution of .0001° C.

Fig. 1. *New linear Quartz Thermometer (foreground) uses quartz resonator as sensor to measure temperatures from −40°C to +230°C at resolutions up to .0001°C. Thermometer can measure temperature at many-meter distances, and digitally-presented data can be recorded and processed by existing hardware. One calibration point of Thermometer is established by freezing-point of tin (+231.88°C).*

IT HAS LONG been recognized that the temperature dependence of quartz crystal resonators was a potential basis for the accurate measurement of temperature. In practice, however, it has not previously been satisfactory to make wide-range temperature-measuring systems based on quartz resonators because of the large non-linearity in the temperature coefficient of frequency of available quartz wafers. Recently, however, an orientation in quartz was predicted and verified by Hammond[1] in the –hp– laboratories which resulted in a crystal wafer having a linear temperature coefficient over a wide temperature range. This new orientation, the "LC" (linear coefficient) cut, has permitted development of a "quartz thermometer" that measures temperatures automatically, quickly, and with very high resolutions on a direct digital display. Temperatures can be measured over a range from −40°C to +230°C to a resolution of .0001°C in 10 seconds —or faster with proportionately less

SEE ALSO:
Simplified presentation of transistor noise performance, p. 8

Fig. 2. *Two-channel version of Quartz Thermometer can measure temperature sensed by either probe or difference between probes. Sensor oscillator is normally located within cabinet but is self-contained and can be located externally for remote measurements.*

resolution or in repetitive measurements.

Two versions of the thermometer have been designed, one of which has two inputs to enable differential measurements of temperature. The two versions of the instrument have each been designed to read directly in Fahrenheit (−40°F to +450°F) or in Centigrade (Celsius) but not both.

It is apparent on its face that a temperature-measuring instrument with the above capabilities has great value in many fields, but the instrument also has a number of additional characteristics that are of much interest. It is possible, for example, for the instrument to make measurements through connecting wires at distances of up to 10,000 feet, with no adverse effect on measurement accuracy caused by lead length. Other unusual and interesting characteristics are discussed later.

The thermometer's temperature-sensing quartz resonator is located in a small sensor probe which connects through a length of cable to its oscillator. The oscillator is located in the main cabinet but can be physically removed as a unit to permit measuring temperatures at a distance from the cabinet. The cabinet otherwise contains what is essentially a special frequency counter which displays the measured temperature directly in numerical form on a digital readout. The temperature measurements are made automatically, either repetitively or initiated singly with a panel push button in the manner of a frequency counter. Repetitive readings can be made from 4 per second to 1 per 15 seconds. Three styles of sensor probes have been designed to accommodate various measurement situations including measurements in high-pressure environments. The time constant of each of the probes is only 1 second.

RESONATOR TEMPERATURE COEFFICIENT

Quartz wafers are widely used in oscillator circuits to hold the operating frequency constant. In this application, temperature has been the principal factor influencing the stability of quartz resonators. It was discovered some time ago, however, that the temperature coefficient of frequency is both a function of the angle at which the resonator is sliced from the parent crystal and of the temperature itself. In 1962, Bechmann, Ballato and Lukaszek of the U. S. Signal Corps Lab, at Ft. Monmouth, N. J. reported an analysis of the first, second, and third order temperature coefficients of frequency of a number of quartz resonator designs.[2] This analysis made it possible to calculate the first three coefficients of a third-order expansion of the temperature-dependent frequency for a quartz crystal plate of generalized orientation:

$$f(T) = f(0)(1 + \alpha T + \beta T^2 + \gamma T^3)$$

Bechmann used this approach to study resonator orientations with a zero first-order temperature coefficient ($\alpha = 0$).

Recently, Hammond, Adams, and Schmidt[1] of the Hewlett-Packard Company used this same approach to determine that an orientation existed in which the second and third order terms went to zero ($\beta = \gamma = 0$) while the first order term remained finite. This orientation occurred for a thick-

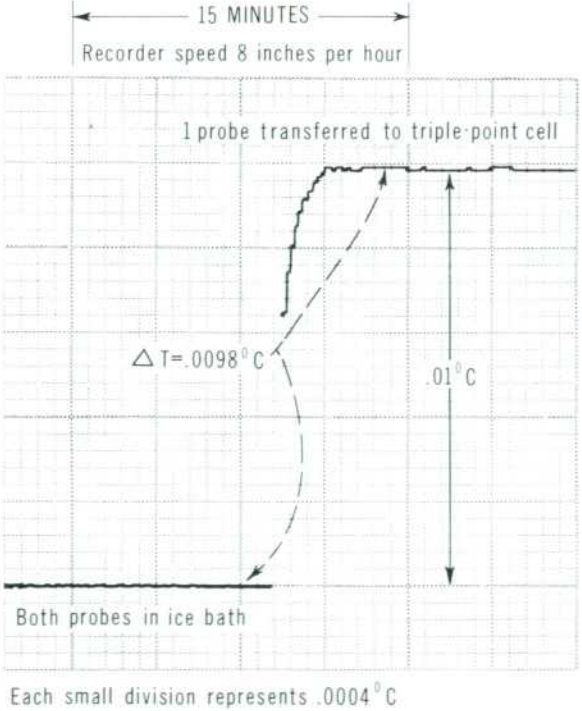

Fig. 3. *Recording of measurement made with two-channel Quartz Thermometer of difference between melting point of ice and triple-point of water. By definition, the latter is +.01° Celsius (Centigrade) and is considered to be .01° above ice melting point.*

ness-shear mode of operation designated the "LC" cut, for Linear Coefficient of frequency with temperature. This cut is the basis for the sensor design used in the new Quartz Thermometer.

Resonators sliced in the LC orientation from high-quality synthetic single-crystal quartz exhibit a temperature coefficient of 35.4 ppm/°C. For use in the new thermometer, the resonators are ground to the precise thickness and orientation required to achieve the linear mode while exhibiting a frequency slope of 1000 cps/°C. This slope is achieved at a third overtone resonance near 28 Mc/s.

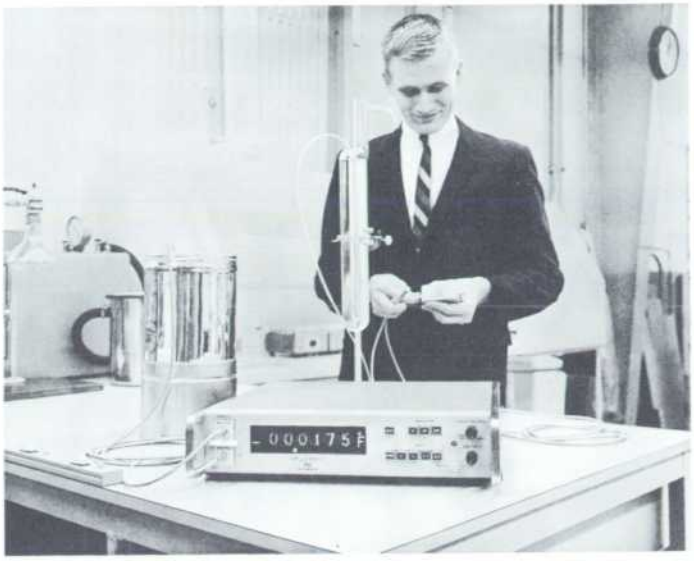

Fig. 4. *Two-channel Quartz Thermometer measuring a small temperature difference. Six-digit display permits such difference measurements to be measured with a resolution of .0001°C.*

QUARTZ PROPERTIES

Quartz-crystal wafers have certain desirable properties which make them valuable as resonators in frequency standards and time-keeping systems and which are equally important for temperature-sensing systems. Chief among these are quartz's high purity and chemical stability. Further, quartz is a hard material that cannot be deformed beyond its elastic limit without fracture. It has almost perfect elasticity and its elastic hysteresis is extremely small.

THE LINEAR COEFFICIENT QUARTZ RESONATOR

For digital thermometry, the ideal quartz crystal resonator should have a linear frequency-temperature characteristic. This characteristic can be well-represented over rather wide temperature ranges for nearly all types of quartz resonators by a third-order polynomial in temperature. The two degrees of orientational freedom which are significant in quartz resonators are just sufficient to adjust the second- and third-order terms to zero if a region of solution exists.

An analysis was made of the frequency temperature behavior of the three possible thickness modes for all possible orientations in quartz using Bechmann's constants.[1] A single orientation of wave propagation was found for which the second- and third-order temperature coefficients are simultaneously zero. The accompanying diagram shows the analytically-determined loci of zero second-order and third-order temperature coefficients for the lowest frequency shear mode, the C mode, in a primitive orientational zone in quartz. These loci cross at $\phi = 8.44°$ and $\theta = 13.0°$. Experimental studies indicate the actual orientation of zero second- and third-order terms to be $\phi = 11.17°$ and $\theta = 9.39°$. The discrepancy between observed and predicted orientations is consistent with the accuracy of the elastic and expansion constants used in the analysis. A resonator cut at this orientation and operated on the C mode, has been designated the **LC** cut to indicate **L**inear **C**oefficient of frequency with respect to temperature.

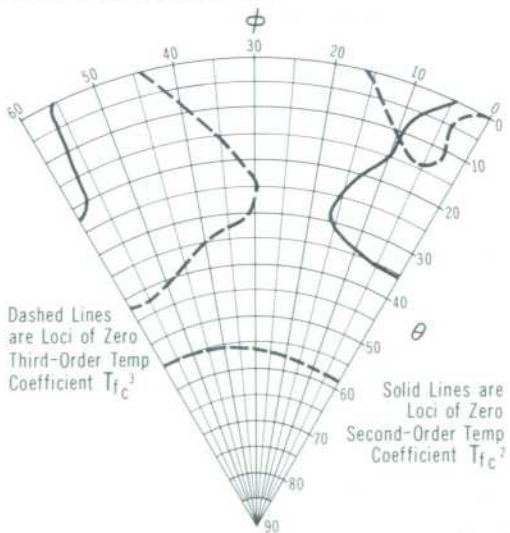

Analytically-determined loci of zero second-order (solid lines) and third-order (dashed lines) temperature coefficients for C mode in primitive orientational zone in quartz.

At this orientation, the nonlinearity is restricted to the fourth- and higher-order terms which have been experimentally shown to be less than a few millidegrees over the temperature range from 0 to 200°C.

It is interesting to note that the frequency-temperature relationship was linearized with respect to the International temperature scale. If a new temperature scale is adopted in the future, minor adjustments can be made in the two orientational parameters of the LC cut to linearize relative to the new temperature scale. —*Donald L. Hammond*

[1] R. Bechmann, A. D. Ballato, and T. J. Lukaszek, "Higher Order Temperature Coefficients of the Elastic Stiffness and Compliances of Alpha Quartz," **Proc. IRE,** Vol. 50, No. 8, August, 1962.

Fig. 5. *Close-up view of quartz sensor mounted on header. Sensor is later sealed in helium atmosphere.*

Quartz, unlike the platinum or nickel used in resistance thermometers, can be found in a natural state that has a high degree of purity. Alpha quartz, the crystalline formation that exhibits a piezo-electric effect, is generally found in Brazil, but American-made synthetic quartz is now available. Both exhibit impurity levels of less than 10 ppm (an almost negligible amount). Its ordered crystalline structure resists the plastic deformation that causes drift and retrace errors in resistance materials and permits the great frequency-stability found in quartz crystal resonators. The short-term variations of indicated temperature in the quartz thermometer, for example, are much less than .0001°C.

Quartz's asymmetrical structure also provides control of its temperature characteristic through angular orientation that is unavailable in the amorphous resistance materials. Platinum, for example, has a fixed deviation from the best straight line of .55% over the same range as the quartz thermometer, which is currently held to less than .05%.

SENSOR CONSTRUCTION

After the deposition of gold electrodes on the surface of the quarter-inch diameter quartz wafer, each wafer is brazed to three small ribbons which support it inside a TO-5 size transistor case (Fig. 5). Thus mounted, the quartz is remarkably immune from both drift and breakage. Drop tests have shown that an acceleration of more than 10,000 g's is required to fracture the crystal, and that no discernible shift in calibration occurs short of the point of fracture. Vibration levels of 1000 g's from 10 c/s to 9000 c/s have had no measurable effect.

The wafer case is hermetically sealed in a helium atmosphere which provides both a good heat conduction path and a passive atmosphere for long term resonator stability. The wafer itself dissipates only 10 μW internally, an amount of heat that contributes less than 0.01°C error when the sensor is in water flowing at 2 ft./sec.

Since slope and linearity are controlled closely during manufacture by the orientation and thickness of the crystal and its gold electrodes, quality control is more precise than is possible with resistance thermometer materials. No detectable change in slope or linearity after manufacture has occurred in crystals tested to date. There is a characteristic "aging" effect that causes the frequency (measured at the ice point) to change about 0.01°C per month but, because no slope changes occur, recalibration at the ice point alone is usually sufficient.

FREQUENCY TO DIGITAL CONVERSION

The block diagram of the new thermometer in Fig. 6 shows how electronic counter techniques are used with the quartz resonator/oscillator to obtain a digital display of temperature.[3, 4] The sensor oscillator output is compared to a reference frequency of 28.208 Mc/s. By design, this frequency is also the sensor frequency at zero degrees. As mentioned previously, the frequency of the quartz sensor was chosen so that a slope of 1000 cps/°C is obtained, i.e., a temperature of 200°C produces a sensor frequency that differs from the reference by 200 kc/s. The difference frequency is detected in the mixer circuit, converted into a pulse series and passed to the electronic display decades. Here, it is counted for a fixed length of time and the resulting count is displayed on "Nixie" tubes to provide a numerical readout.

The duration of the count is controlled by the reference oscillator, which drives the gate control-circuit through a frequency divider chain. The count accumulates at a rate of 1000 c/s per second per °C difference from 0°C. The counting or gating interval then determines the resolution.

The optional Fahrenheit scale is obtained by increasing the gate-time by a factor of 9/5 and using a reference crystal 1.778 kc/s lower in frequency than the Centigrade unit. This lower frequency reduces the zero-reading point by 17.78°C, equivalent to 32°F.

The reference crystal is mounted in a temperature-controlled oven to achieve a long-term drift of only a few parts in 10^7 per month, or less than 0.005°C change in zero-setting per month. Short-term stability is such that changes from reading to reading

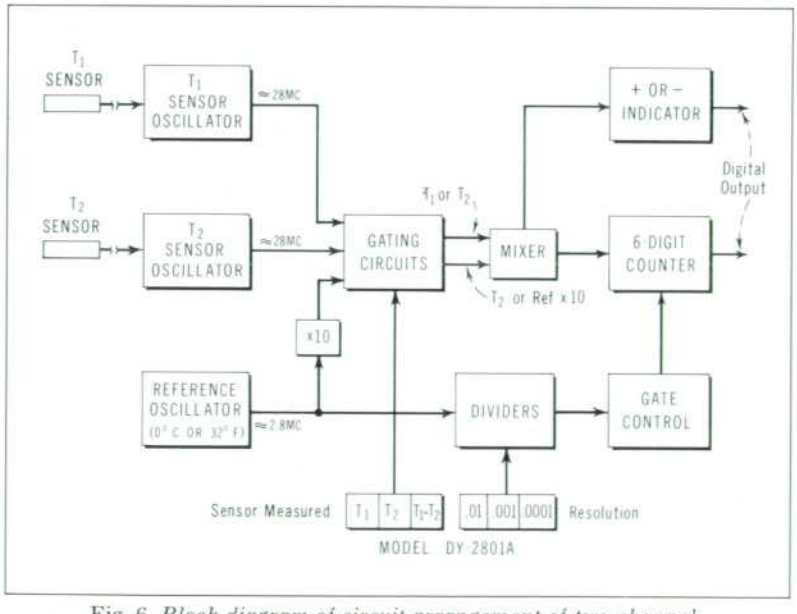

Fig. 6. *Block diagram of circuit arrangement of two-channel Thermometer. Single-channel Thermometer circuit is similar in principle but does not include second sensor channel, variable gate times, or difference-temperature capability.*

are less than 0.2 millidegrees, unnoticeable on the 4-digit instrument and noticeable only when using the 0.0001° resolution scale of the dual-channel instrument.

DIFFERENTIAL TEMPERATURE MEASUREMENTS

The higher resolution of the two-channel unit over the single-channel unit has been achieved by using a 6-digit readout and longer gating (sampling) intervals than the 0.01 second of the single-channel instrument. In the two-channel unit, one of three gating intervals can be selected by front panel push buttons. The 0.1-second gate provides temperature measurements in least increments of one-hundredths of a degree, the 1-second gate millidegree increments, and the 10-second gate tenths of millidegrees.

In this instrument, the preset number in the time base dividers is adjustable with decade switches on the rear of the instrument. These provide a means of compensating for variations in the frequency/temperature slope of individual probes during the calibration of the instrument. Being a digital technique, the adjustment is not a potential source of drift error. The two probes normally are supplied with slopes matched to better than 0.05%. The zero temperature frequencies are matched closely enough so that trimmers on the individual sensor oscillators can provide an exact zero indication.

The two-channel instrument, which can be programmed externally, may be switched to indicate the absolute temperature sensed by either probe. Differential temperature measurements are obtained by switching the instrument to measure the beat frequency between the two sensor oscillators.

To identify on which side of zero the measured temperature lies, the two-channel instrument has a polarity indicator circuit that compares the sensor oscillator output to the reference frequency. The comparison determines which signal is higher in frequency and turns on a "+" or "—" indicator accordingly. In the differential mode, the polarity indicates whether probe T_1 is higher than or lower than probe T_2. The polarity indicator can also be incorporated in the single-channel unit.

Fig. 7. *Single-channel Thermometer. Sensor oscillator can also be used externally for remote measurements.*

SENSOR PROBES

The outer shell of the three sensor probes is fabricated from type 304 stainless steel for chemical stability. In these probes the quartz wafer is situated parallel to and about .01 inch away from the flat circular end of the probe and is sealed in a helium atmosphere, as mentioned previously. The 12-foot connecting cable has a dielectric and outer sheath of type TFE Teflon which can withstand temperatures up to 250°C. The stainless steel shell on the probes is thin and of small diameter, resulting in a low thermal mass of less than 10^{-3}BTU/°F (equivalent in heat capacity to less than 0.5 gm of water) for the short probe.

The low thermal conductivity of the thin-wall shell also results in a low value of stem conduction error. This error is, for example, less than 0.01% of the temperature difference between the tip and the threaded end of the longer probe as measured in essentially stationary water.

Much work has also been done in the design of the probes to achieve a low thermal time constant, which is less than 1 second as measured in warm water moving at 3 fps.

The two longer probes are equipped at the cable end with a fitting that adapts the probes for insertion into pipes and tanks. The fittings have a standard ¼" National Pipe Thread. All probes may be used in pressures up to 3,000 psi.

SENSOR OSCILLATOR

The sensor oscillator is in a small die-cast aluminum case, as shown in Fig. 2, with a waterproof coaxial connector at each end. DC power for the oscillator is supplied over the same cable that carries the oscillator frequency back to the instrument. The solid-state oscillator may be operated within a temperature range of —20°C to +70°C and shifts the indicated temperature by less than 0.001° per degree of ambient change. A trimmer is provided to shift the frequency of the oscillator slightly (±50 cps) so that a pair of probes can be exactly matched.

The oscillator-amplifier combination provides virtually complete isolation between the sensor and any variations due to cable length and load. When some distance is required between the point of measurement and the instrument, a standard 70-ohm coaxial cable can be used for an extension; losses as high as 20 dB can be tolerated which permits a cable length, using RG-59/U, as great as 1000 ft. For greater extensions, lower loss cables or booster amplifiers can be used, and it appears likely that lengths beyond 10,000 feet are entirely feasible.

The cable between the sensor and oscillator is necessarily fixed at ½ wavelength of 28 Mc/s to reflect the crystal impedance directly to the oscillator.

DIGITAL OUTPUT

An additional advantage of Quartz Thermometers is that the measurement information is provided in a digital form that is readily recorded or

Fig. 8. *Quartz Thermometer (upper unit) used with Scanner and Printer to measure and record up to 100 temperatures. Measurements can be recorded on paper tape as shown, or on punched tape, cards or magnetic tape.*

transmitted for processing. BCD outputs for direct coupling into digital recorders, such as the –hp– Model 562A, are included.

Analog records such as that shown in Fig. 3 may be obtained by using a strip-chart recorder in conjunction with the analog output from the –hp– Model 562A Printer or the Model 580A Digital-Analog Converter.

REMOTE SENSING

Since the sensor oscillator output is a frequency-modulated radio-frequency signal, it opens the possibility for telemetric transmission by direct radiation from the sensor oscillator alone at the 28.2 Mc/s frequency. Transmission in the range of existing telemetry receivers may be had by multiplying the frequency four times to 112.8 Mc/s. Telemetry receivers can be made to provide a frequency output proportional to temperature by using the quartz thermometer reference oscillator as a beat frequency oscillator (BFO) and coupling the output signal to an electronic counter. In this way one can realize the full precision of the Thermometer.

The ability of the Quartz Thermometer to transmit data in FM form over long cable runs also opens the possibility of improved precision in measuring temperatures at great depths and at many points in the ocean. The measurement information could be transmitted either by the extended cable connection mentioned above or by radio telemetry from floating buoys.

RATE INPUT

Since the Quartz Thermometer has all the elements of an electronic frequency counter, it was convenient to arrange the two-channel instrument for use as a frequency counter. A separate input terminal and a sensitivity control for input signals are on the front panel, and a front panel switch converts the instrument to a frequency counter having a maximum counting rate of 300 kc/s.

CALIBRATION TECHNIQUES

The temperature-sensing quartz resonators are calibrated after being sealed in their cases but prior to mounting in probe shells. Calibration is accomplished by mounting each res-

BRIEF SPECIFICATIONS

-dy- MODELS 2800A and 2801A

QUARTZ THERMOMETERS

TEMPERATURE RANGE: –40 to +230°C (–40 to +450° F with Option M1).

RESOLUTION:

MODEL NO.	READING① RESOLUTION ("C or °F)	FULL SCALE DISPLAY °C Readout	FULL SCALE DISPLAY °F Readout	SAMPLE PERIOD (Sec.) °C	SAMPLE PERIOD (Sec.) °F
2800A	.1	230.0	450.0	.01	.018
2801A	.01	0230.00	0450.00	.1	.18
	.001	230.000	450.000	1.0	1.8
	.0001	*(2)30.0000	*(4)50.0000	10.0	18.0

① ±1 digit ambiguity in least significant displayed digit for all sample periods.

* 'Hundreds' digit not displayed when using .0001° resolution.

ACCURACY: Best accuracy determined by 'Linearity' and 'Short-Term Stability,' listed below.

LINEARITY (ABSOLUTE): Better than ±.02°C (.04°F) from 0 to +100°C, referred to straight line through 0 and 100°C. Better than ±.15°C (.27°F) from –40 to +230°C, referred to straight line through 0 and 200°C.

MATCHED PROBES: With DY-2801A, probes are matched to better than ±.1°C at 200°C, or .05% of operating temperature (when zero set at icepoint).

STABILITY

SHORT-TERM: Maximum variation from reading-to-reading at constant probe temperature less than ±.0002°C (.0004°F) for absolute measurements. No reading-to-reading variation for differential measurements (excluding normal display ambiguity of ±1 count in least significant digit).

LONG-TERM: Zero drift less than ±.01°C (.018°F) at constant probe temperature for 30 days.

TEMPERATURE CYCLING: When used repeatedly over range from –40 to +230°C, reading at 0°C will not change by more than ±.05°C (.09°F). Error decreases with reduced operating range.

AMBIENT TEMPERATURE: Reading changes by less than .001°C per °C change in ambient temperature for instrument or sensor oscillator.

RESPONSE TIME: Response to step function of temperature, measured by inserting probe into water at dissimilar temperature flowing at 2 fps:

63.2% of final value in <1.0 sec.
99.0% of final value in <4.5 sec.
99.9% of final value in <6.9 sec.

THERMAL MASS:

DY-2850A (SHORT) PROBE: Equivalent to less than 0.5 gm of water.

SELF-HEATING: Less than 10μw; contributes less than .01°C error with probe immersed in water flowing at 2 fps.

INTEGRATION TIME: Defined by sample period selected; see 'Resolution.'

SAMPLE RATE: Readings are taken in response to pushbutton or external signal, or automatically at self-regulated intervals. Time interval between readings can be adjusted at front panel from approximately .2 to 5 sec.

POWER REQUIRED: 115/230 v ±10%, 50 to 60 cps { DY-2800A, 65 w. / DY-2801A, 85 w.

PROBE ENVIRONMENT:

MEASURAND: Gases and liquids non-reactive with 304 stainless steel. Probes can be supplied in other materials such as 316 stainless steel on special order.

TEMPERATURE: –200 to +250°C (–330 to +480°F). Instrument zero may require readjustment on returning to proper operating range from temperatures below about –100°C.

PRESSURE: 3000 psi maximum.

SHOCK: To 10,000 g, without change in calibration. Equivalent to 10-inch drop onto steel surface.

VIBRATION: To 1000 g at 1000 cps.

NUCLEAR RADIATION:

X-Ray or Gamma Radiation: Levels to 10^8 roentgens are permissible. Radiation at this level may cause a frequency offset in the order of 1 ppm, which can be removed by heating probe to +250°C.

Neutron Radiation: Low energy (e.g. .025 ev) thermal neutrons will not affect crystal. Higher energy neutron radiation can be expected to cause permanent damage to crystal.

SENSOR OSCILLATOR ENVIRONMENT: Ambient temperatures from –20 to +70°C (–4 to +158°F). May be totally immersed; constituent materials are aluminum, nickel, neoprene, Teflon, epoxy paint.

INSTRUMENT ENVIRONMENT: Ambient temperatures from 0 to +55°C (+32 to +130°F), at relative humidity to 95% at 40°C.

PRICE:

MODEL DY-2800A QUARTZ THERMOMETER: With one Temperature Sensor, Model DY-2850C (unless otherwise specified), $2,250.

MODEL DY-2801A QUARTZ THERMOMETER: With two Temperature Sensors, Model DY-2850C (unless otherwise specified), $3,250.

Prices f.o.b. Palo Alto, California

Data subject to change without notice

Fig. 9. *Sensor probes presently designed for Quartz Thermometer. Probes can be use in pressures up to 3,000 psi. Fittings on longer probes facilitate measurements in tanks, pipes, etc.*

onator case in a test probe and operating these in groups of 50 in a temperature-controlled oil bath.

Each probe is connected to a separate sensor oscillator, and the oscillators are scanned by a scanner similar to the one in Fig. 8. The frequencies of the resonators are printed sequentially on an –hp– 562A Recorder at each calibration temperature.

Eight calibration temperatures are used ranging from —40°C to +240°C in 40° steps. The calibration baths are monitored by a transfer standard calibrated against an NBS-certified platinum resistance thermometer and Mueller bridge. The transfer standard is regularly checked for drift in a triple-point cell, a certified tin-freezing-point standard, and against the freezing point of triple-distilled mercury. If excessive drift is noted, the transfer standard can be recalibrated against the certified thermometer. These checks, plus the excellent short-term stability of the temperature-controlled baths, achieve a calibration accuracy of 0.01°C at all eight points.

The crystals are individually classified into groups on the basis of the zero degree frequency and the average slope. The grouping permits the matching of probes for use in the dual-channel instrument.

The data for each sensor are applied to a computer program which provides preset numbers for the best average slopes to use over both the 0°C to 100°C range and the full —40°C to +230°C range. The computer also prints a table of deviations for each range in 10° steps so that corrections for the residual non-linearity can be applied in critical applications to the displayed readings. The maximum deviations permitted are 0.02°C for the 0°–100° range and 0.15°C for the full range of the instrument.

ACKNOWLEDGMENT

The design of the Quartz Thermometer is based on the development of the linear coefficient quartz resonator by Donald L. Hammond in the –hp– Physics R and D Laboratory. Herschel C. Stansch as project manager was responsible for the instrument development. The members of the design team included Cleaborn Riggins, John M. Hoyte, Kenneth G. Wright, F. Glenn Odell, Willis C. Shanks, and Malcolm W. Neill. We also wish to acknowledge the services of Donald E. Norgaard and Robert J. Moffat.

—Albert Benjaminson

REFERENCES

[1] D. L. Hammond, C. A. Adams, P. Schmidt, Hewlett-Packard Co., "A Linear Quartz Crystal Temperature Sensing Element," presented at the 19th Annual ISA Conference, Oct. 12-15, 1964, New York. **Preprint No. 11, 2-3-64.**

[2] See footnote in separate article, p. 3.

[3] H. C. Stansch, "A Linear Temperature Transducer with Digital Readout" presented at the 19th Annual ISA Conference, Oct. 12-15, 1964, New York. **Preprint No. 11, 2-2-64.**

[4] Albert Benjaminson, "The Quartz Crystal Resonator as a Linear Digital Thermometer," presented at 4th Annual Conference of the Temperature Measurements Society, Feb., 1965.

DESIGN LEADERS

Donald L. Hammond

Don Hammond joined –hp– in 1959 as manager of the Quartz Crystal Department where he established the –hp– facility for precision quartz-crystal resonator production. Don participated in the research and development which led to the high-precision resonators in the –hp– 106A and 107A Quartz Oscillators and the crystal "flywheel" used in the –hp– 5060A Cesium Beam Frequency Standard, and he also developed the linear quartz temperature sensor. In 1964, Don was transferred to the position of general manager of the –hp– Physics R & D group where he directs research and development on quantum-electronics, electro-acoustics, and high-vacuum devices.

Don received BS and MS degrees in Physics from Colorado State University and has done further graduate study at Columbia University. He has also directed research in industry and at government laboratories in the areas of frequency-control devices, synthesis of crystalline quartz, solid-state properties of quartz, and the theory of vibrations applied to piezo-electric resonators.

Albert Benjaminson

Al Benjaminson joined the Hewlett-Packard Dymec Division in 1959 as a development engineer. He was made Engineering Manager of RF System Development in 1960 and in this position was responsible for the Dymec 5796, 2650, and 2654 Oscillator Synchronizers, for the 2590 Microwave Frequency Converter, and for the 2365 Tunable VLF Receiver. In 1964 he was made Engineering Manager for transducer development in which capacity he is responsible for the Quartz Thermometer development.

During World War II, Al was stationed at the Naval Research Lab, Radio Materiel School in Washington as an electronics instructor. He attended the Polytechnic Institute of Brooklyn on a part-time basis and then obtained his BEE degree at the University of Adelaide, South Australia, during the post-war years. He has worked as a radio design engineer on commercial products and was also an engineering section head for military airborne electronic systems before joining Dymec.

THE INFLUENCE OF TRANSISTOR PARAMETERS ON TRANSISTOR NOISE PERFORMANCE — A SIMPLIFIED PRESENTATION

Some factors that define the noise characteristics of junction transistors have been investigated and are presented here in graphic form. The data illustrate the magnitude of the noise parameters and their variation with operating point.

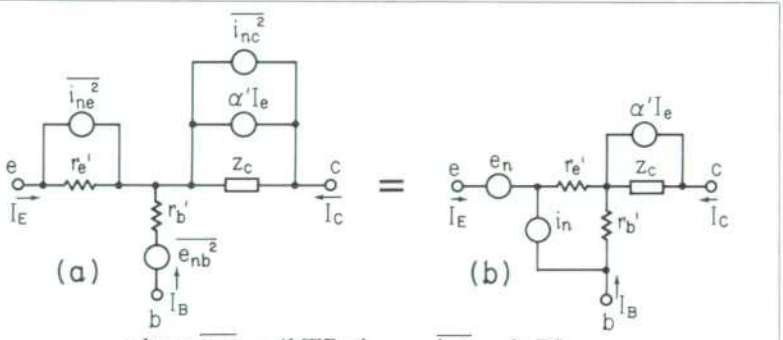

where $\overline{e_{nb}^2} = 4kTBr_b'$ $\quad \overline{i_{ne}^2} = 2qBI_E$

$$\overline{i_{nc}^2} = 2\alpha_o(1-\alpha_o)qBI_E F(f) + 2qBI_{co}$$

$$\text{and } F(f) = \frac{1 + \left(\dfrac{f}{f_\alpha\sqrt{1-\alpha_o}}\right)^2}{1 + (f/f_\alpha)^2}$$

Fig. 1(a). *Noise model of a junction transistor in which the noise-producing mechanisms of the transistor are represented in the T equivalent-model by three uncorrelated noise generators. The noise generator $\overline{e_{nb}^2}$ represents the thermal noise in the base resistance r_b', the noise generator $\overline{i_{ne}^2}$ represents shot and thermal noise in the emitter-base diode, and the noise generator $\overline{i_{nc}^2}$ represents the noise in the collector-base junction.*

Fig. 1(b). *Noise model of a junction transistor in which the sources of noise within the device are represented by an external noise voltage generator e_n and an external noise current generator i_n. The magnitude of each of these generators is determined from the magnitudes of the noise generators of Nielsen's model.*

Noise in junction transistors is basically a consequence of the motion of charge carriers in the semiconductor material. The processes to which the noise characteristics can be attributed have been defined by A. van der Ziel[1] and have been incorporated into the T equivalent circuit of the transistor by Nielsen.[2] For an NPN transistor, the noise producing mechanisms which define the noise characteristics of junction transistors are:[3]

1. noise due to electrons passing from emitter to collector,
2. noise due to electrons passing from emitter to base,
3. noise due to electrons injected into the base returning to the emitter,
4. noise due to electrons trapped in the emitter space-charge region recombining with holes coming from the base,
5. noise due to electrons trapped in the emitter space-charge region returning to the emitter after being detrapped thermally, and
6. thermal noise due to the extrinsic base resistance r_b'.

The effect of these noise mechanisms was introduced by Nielsen into the T model of a junction transistor in the form of three uncorrelated noise generators as shown in Fig. 1 (a).

In this model,[4] the noise generator $\overline{e_{nb}^2}$ represents the thermal noise in the base resistance r_b', the noise generator $\overline{i_{ne}^2}$ represents shot and thermal noise in the emitter-base diode, and the noise generator $\overline{i_{nc}^2}$ represents the noise in the collector-base junction. The purpose of this discussion is to transform the noise sources of this model into a form which may more readily be evaluated experimentally and which may be more clearly interpreted to determine the effect of transistor operating point and transistor parameters on noise performance.

INTERPRETATION OF NOISE MODEL

A noisy twoport, i.e., one with internal noise-generating mechanisms, can be represented as a noiseless twoport with external noise generators. This transformation can be applied to Nielsen's model and these internal noise sources can be represented by an external noise-voltage generator e_n and an internal noise-current generator i_n, as shown in Fig. 1 (b).

To assure the equivalence shown in Fig. 1, the values of the noise generators e_n and i_n are determined by matching the terminal properties of the two models of the transistor. Under the as-

[1] A. van der Ziel, "Shot Noise in Transistors," **Proc. IRE**, Vol. 48, pp. 114-115, January, 1960.

[2] E. G. Nielsen, "Behavior of Noise Figure in Junction Transistors," **Proc. IRE**, Vol. 45, pp. 957-963, July, 1957.

[3] These statements are formulated in terms of the majority carriers (electrons) for an NPN device merely for simplicity. The processes are equally applicable to PNP transistors upon the appropriate substitution of the majority carriers (holes) for the PNP transistor.

[4] This noise model does not include the effect of 1/f noise; consequently, this discussion is limited to the frequency range above the 1/f noise region which is typically below 1 kc.

sumption that $Z_c >> r_b'$ and $Z_c >> r_e'$, the mean-square magnitudes of e_n and of i_n are:[5]

$$\overline{e_n^2} = 2kTBr_e' + 4kTBr_b' + \frac{2kTB\,(r_e' + r_b')^2\,F_1(f)}{\beta_o r_e'} \qquad (1)$$

$$\overline{i_n^2} = \frac{2kTB}{\beta_o r_e'}\,F_1(f) \qquad (2)$$

where $F_1(f) = 1 + \left(\frac{f}{f_\alpha\sqrt{1-\alpha_o}}\right)^2$

for the common-base and the common-emitter configurations, and

$$F_1(f) = \frac{1 + \left(\frac{f}{f_\alpha\sqrt{1-\alpha_o}}\right)^2}{1 + (f/f_\alpha)^2}$$

for the common collector configuration.

The magnitude of the noise-voltage generator e_n is composed of terms derived from each of the noise generators found in Neilsen's model. The noise current is a result of the collector current-generator $\overline{i_{nc}^2}$ which represents the noise in the collector-base junction of the transistor.

GRAPHIC PRESENTATION OF e_n AND i_n

The variation in the magnitude of these two noise generators with the operating point (I_E) provides an insight into the noise properties of transistors. This variation is graphically presented in Figs. 2 and 3 in which $\sqrt{\overline{e_n^2}}$ and $\sqrt{\overline{i_n^2}}$ are plotted on a per square-root cycle basis as a function of emitter current. The frequency dependence of $\overline{e_n^2}$ and of $\overline{i_n^2}$ shown in Equations 1 and 2 is neglected for this presentation.

The magnitude of the noise-voltage generator e_n is an asymptotic approximation based upon the dominant term of the expression for $\overline{e_n^2}$ of Equation 1.

[5] These expressions are approximately true for all configurations, but exact only for the common-base and common-emitter configurations. The noise contribution of I_{CO} is neglected in this discussion.

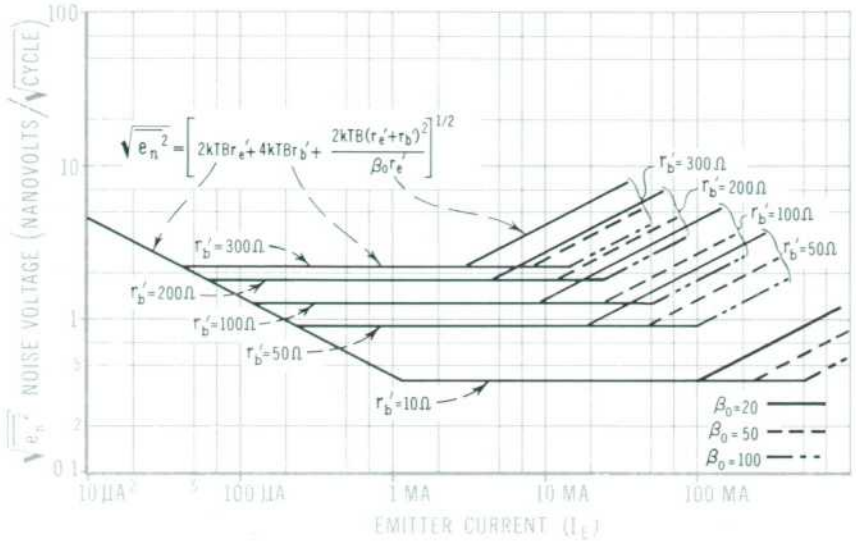

Fig. 2. *Asymptotic representation of the variation in the magnitude of the noise-voltage generator e_n with emitter current with r_b' and β_o as running parameters. Variation presented for a temperature (T) of 290°K.*

In the graphical presentation, three regions of interest are apparent. In Region I, i.e., the left-hand portion of the curve in which $\sqrt{\overline{e_n^2}}$ is denoted by a single line of negative slope, the magnitude of e_n is determined by the noise associated with the emitter-base diode in Nielsen's model. In Region II, in which $\sqrt{\overline{e_n^2}}$ is denoted by a series of horizontal lines (one for each value of r_b'), the magnitude of e_n is determined by the noise associated with the extrinsic base resistance (r_b') of the transistor. In Region III, in which $\sqrt{\overline{e_n^2}}$ is denoted by a series of lines of positive slope, the magnitude of e_n is determined by the noise associated with the collector-base diode and is strongly influenced by the value of β_o of the transistor. The magnitude of the noise-current generator i_n as shown in Fig. 2 decreases as the emitter current decreases and as the value of β_o for the transistor increases.

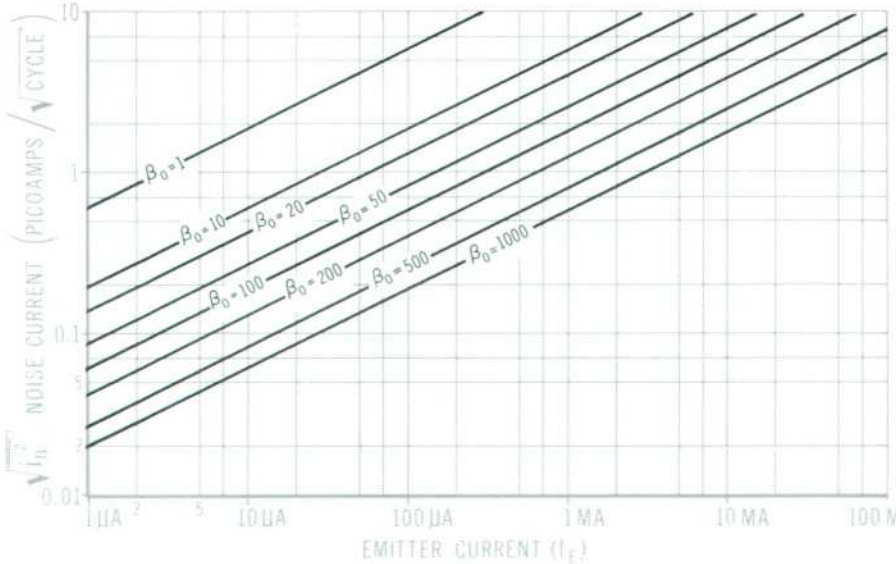

Fig. 3. *The variation in the magnitude of the noise-current generator i_n with emitter current with β_o as a running parameter. Variation presented for a temperature (T) of 290°K.*

NOISE FACTOR OF LINEAR TWOPORTS

In evaluating the noise performance of a twoport, a useful measure is that of noise factor. Noise factor is a measure of the deterioration of the ratio of signal power to noise power as the signal passes through a noisy twoport. Noise factor can also be considered as a measure of the noisiness of a twoport relative to the noisiness of the source

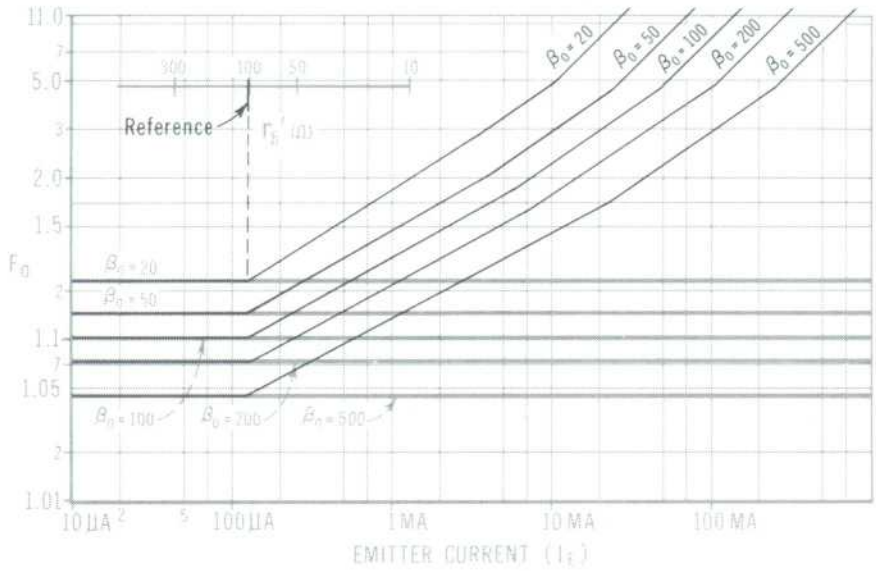

Fig. 4(a). *Dependence of the optimum value of noise factor (F_o) on the emitter current with r_b' and β_o as running parameters. The lowest value of F_o is obtained by biasing the transistor in the low-noise region (below 125 μa for $r_b' = 100\Omega$ as shown in this figure). Presentation constructed for a temperature of 290°K.*

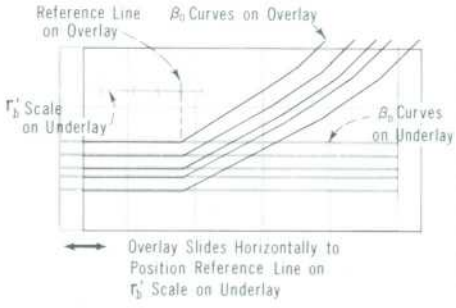

Fig. 4(b). *Illustration of the manipulations required in Fig. 4(a) to show the effect of r_b' upon the positioning of the curves of F_o. The magnitude of r_b' determines the value of emitter current which defines the low-noise region of transistor operation. To show the effect of this parameter, the curves on the overlay are slid horizontally to position the reference line (the junction between Regions I and II) on the desired value of r_b' on the r_b' scale of the underlay. This presentation shows the positioning of the F_o curve for a different value of r_b'.*

driving the twoport. The best possible value of noise factor is unity, i.e., there is no degradation of the input signal-to-noise ratio as the signal passes through the amplifier. For such a case, the twoport would be noiseless and the amplifier could be termed ideal. Noise factor is defined at the reference temperature T_o where $T_o = 290°K$.

An expression for noise factor can be formulated in terms of the magnitudes of the noise-voltage generator and of the noise-current generator. The noise factor (F) of a twoport can be expressed as:[6]

$$F = 1 + \frac{\overline{|i_n + Y_s e_n|^2}}{\overline{i_{sn}^2}} \qquad (3)$$

where $\overline{i_{sn}^2} = 4kT_oBG_s$ (the mean-square noise current associated with the complex source admittance $Y_s = G_s + jB_s$).

Under the assumption that $Y_s = G_s$ and that the correlation between e_n and i_n may be expressed by the real correlation coefficient,[7] γ, this expression becomes

$$F = 1 + \frac{1}{4kT_oB} \times \left[\frac{\overline{i_n^2}}{G_s} + \overline{e_n^2} G_s + 2\gamma \sqrt{\overline{e_n^2}\,\overline{i_n^2}} \right] \qquad (4)$$

Since G_s appears both in the numerator and in the denominator of this expression, noise factor may be optimized (minimized) with respect to the source conductance (resistance) G_s. The optimum value of conductance (G_o) is:

$$G_o = \frac{\sqrt{\overline{i_n^2}}}{\sqrt{\overline{e_n^2}}} \qquad (5)$$

The corresponding optimum value of noise factor (F_o) is:

$$F_o = 1 + \frac{(1+\gamma)}{2kT_oB} \sqrt{\overline{e_n^2}\,\overline{i_n^2}} \qquad (6)$$

GRAPHIC PRESENTATION OF F_o AND R_o

Based upon the foregoing definitions, the optimum value of noise factor (F_o) and the optimum value of source resistance ($R_o = 1/G_o$) can be determined for any transistor. A graphical interpretation of this information is presented in Figs. 4 and 5 as a function of the transistor operating point.

The asymptotic presentation of noise factor F_o in Fig. 4 shows that the value of F_o increases as emitter current is increased. The lowest value of F_o is found in the left hand portion of the graph in which F_o is represented by a sequence of horizontal lines, one for each different value of β_o. This region corresponds to Region I as previously

[6] H. A. Haus and others, "Representation of Noise in Linear Twoports," **Proc. IRE**, Vol. 48, p. 73, January, 1960.

[7] The mean-square sum of two variables is:
$\overline{(x_1 + x_2)^2} = \overline{x_1^2} + \overline{2x_1x_2} + \overline{x_2^2}$
$= \overline{x_1^2} + 2\gamma\overline{x_1x_2} + \overline{x_2^2}$
where $\gamma = \frac{\overline{x_1x_2}}{\sqrt{\overline{x_1^2}\,\overline{x_2^2}}}$ and is assumed to be real.
Based upon this definition, γ represents the magnitude of that portion of the average product of x_1 and x_2 which provides a contribution to the mean-square sum.

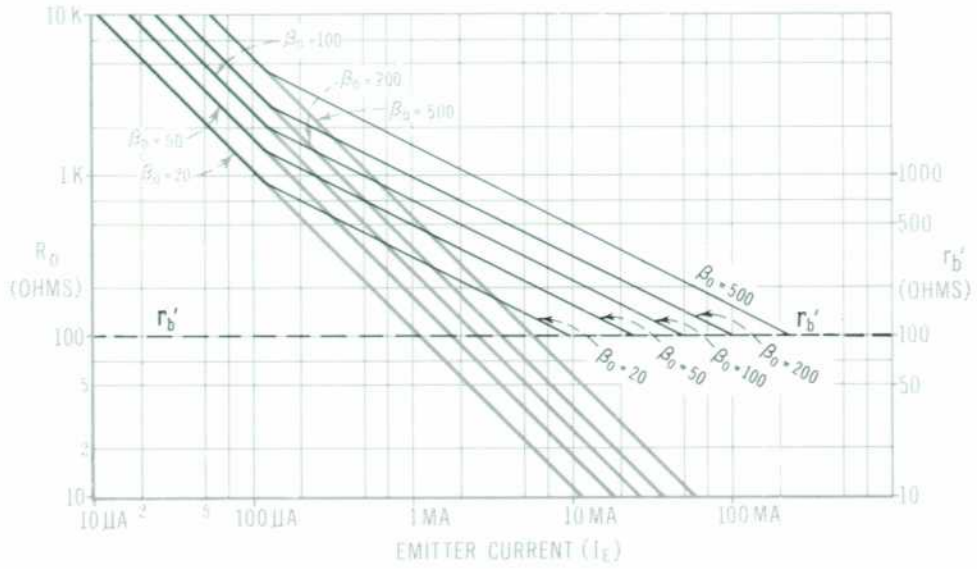

Fig. 5(a). *Dependence of the optimum value of source resistance (R_o) on the emitter current with r_b' and β_o as running parameters. The presentation is positioned for r_b' = 100Ω and is constructed for a temperature (T) of 290°K.*

defined. The next portion of the presentation describes the variation of F_o in Region II and the final portion describes the variation in Region III.

This presentation of F_o provides an insight into the influence of transistor operating point and transistor parameters upon the noise characteristics of a device. The lowest value of noise factor occurs in the region of low emitter current, i.e., in Region I. In this region of low noise,

$$F_o \approx 1 + \frac{1}{\sqrt{\beta_o}} \qquad (7)$$

The point of transition from Region I to Region II is strongly influenced by the value of r_b' since the transition point is defined by the current at which $r_b' = r_e'/2$ (see Fig. 2). This influence of r_b' is shown in Fig. 4 by the r_b' scale appearing at the junction of Regions I and II. This figure is drawn for an r_b' of 100Ω, i.e., the emitter current which defines the transition point is 125μa. If another value of r_b' were selected, this asymptotic curve must be positioned either to the left or to the right by placing the transition point on the appropriate value of r_b' on the scale shown. For large values of r_b', the current which defines this upper boundary of the low noise region is decreased.

Based upon the presentation of Figure 4, a transistor that is to provide low noise amplification should have these properties:

1. a low value of r_b' so that the lowest value of F_o can be obtained at higher currents [a condition which provides higher values for the gain-bandwidth product (f_T) of the transistor]; and
2. a high value of β_o since F_o is inversely proportional to $\sqrt{\beta_o}$.

This presentation indicates the lowest value of noise factor possible for any transistor and the transistor parameters and operating point necessary to realize this optimum value of noise factor.

The optimum value of noise factor can only be obtained when the device is driven with its optimum value of source resistance, R_o. An asymptotic presentation of R_o as a function of emitter current with β_o as a running parameter is shown in Fig. 5. These contours are formed for a value of r_b' of 100Ω. In the same manner as outlined above, this presentation must be positioned to correspond to the particular value of r_b' selected. This approximation to R_o shows that, as the emitter current is increased, R_o decreases. In the low noise region (Region I),

$$R_o \approx r_e' \sqrt{\beta_o} \qquad (8)$$

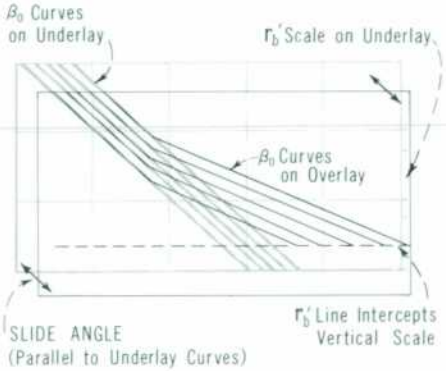

Fig. 5(b). *Manipulations required in Fig. 5(a) to show the effect of r_b' upon the positioning of the curves of R_o. To position the curves of R_o for various values of r_b', the desired value of r_b' is selected on the r_b' scale on the right-hand side of the underlay. The β_o curves of the overlay are positioned so that they coincide with the corresponding β_o curves on the underlay. This positioning of the curves of the overlay defines the variation of R_o with emitter current for any value of r_b' selected.*

SUMMARY

The above graphical representation of $\sqrt{\overline{e_n^2}}$, $\sqrt{\overline{i_n^2}}$, F_o, and R_o provides a clearer insight into the noise characteristics of junction transistors. The asymptotic presentation indicates:

1. the measurable magnitudes of the equivalent noise sources, e_n and i_n;
2. the effect of r_b' in defining the low noise region of transistor operation; and

3. the minimum magnitude of F_o, i.e., $F_o \approx 1 + 1/\sqrt{\beta_o}$.

One final point which is significant in the design of low-noise transistor amplifiers is the effect of variations in source resistance upon the noise factor of the amplifier. The noise factor of a transistor amplifier in terms of the device parameters is:[8]

$$F_o = 1 + \frac{r_e'}{2R_s} + \frac{r_b'}{R_s} + \frac{(R_s + r_b' + r_e')^2}{2\beta_o r_e' R_s} \quad (9)$$

Rewriting this expression as a quadratic equation in the unknown R_s provides a convenient means for determining the range of source resistance over which the noise factor of the amplifier will be less than or equal to a specified value:

$$R_s^2 + R_s[2(r_b' + r_e') - 2\beta_o r_e'(F - 1)] + (r_b' + r_e')^2 + 2\beta_o r_e'(r_b' + r_e'/2) = 0 \quad (10)$$

This expression is graphically presented in Fig. 6 under the stipulation that $r_b' = 100\Omega$ and $\beta_o = 100$ for various values of noise factor (F). The single line curve marked R_o (which intersects the contours of constant noise factor) is the variation of the optimum value of source resistance with operating point. This curve and the asymptotic variation of R_o of Fig. 5 agree quite favorably.

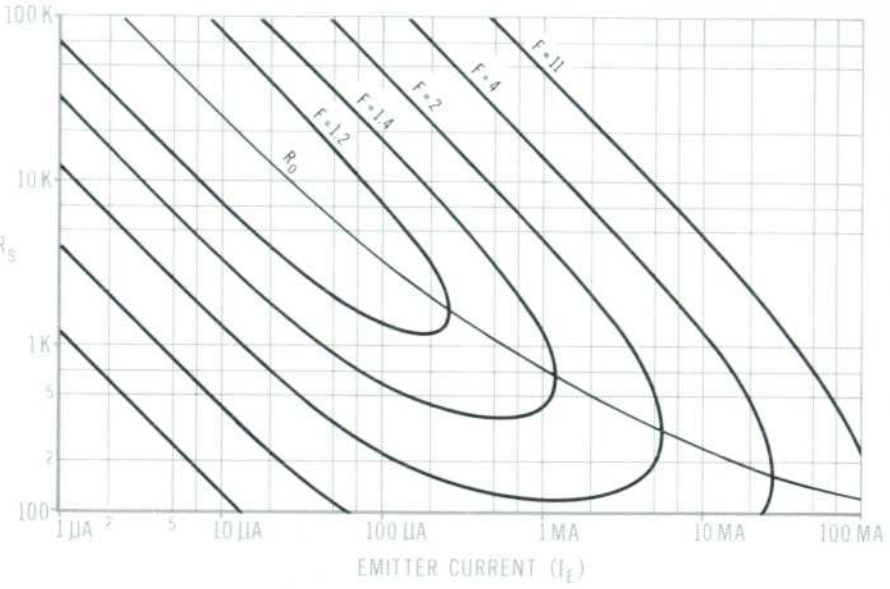

Fig. 6. *Contours of constant noise factor as a function of the resistance of the source driving the transistor and the emitter current of the transistor for $r_b' = 100\Omega$ and $\beta_o = 100$. The single line curve marked R_o is the variation of the optimum value of source resistance with operating point.*

[8] This expression is approximately true for all configurations, but exact only for the common-base and common-emitter configurations.

GENERAL

This discussion has presented some of the factors which define the noise characteristics of junction transistors. The asymptotic interpretation of the noise parameters of the transistor illustrates the magnitude of these parameters and their variation with operating point. This presentation is an interpretation of the noise performance of junction transistors as described by Nielsen's model. The discussion does not consider the influence of 1/f noise on noise performance nor do any of the curves incorporate the high frequency noise characteristics of transistors. The information presented can be applied to any of the three transistor configurations.

ACKNOWLEDGMENT

This discussion is a summary of a portion of a report entitled "The Characterization and Measurement of Noise in Linear Twoports" prepared in the AR and D Division under the auspices of Dr. Paul Stoft. The authors were assisted in the preparation of the above report by Knud Knudsen.

—*Rolly Hassun* and
Michael C. Swiontek

AUTHORS

Michael C. Swiontek

Mike Swiontek has been working on investigative projects in the -hp- Advanced Research and Development Laboratory since joining -hp- in early 1963. A Magna Cum Laude graduate in Electrical Engineering from the University of Detroit, Mike has earned both his MSEE and PhD degrees at Stanford University. He attended Stanford on an International Telephone and Telegraph Fellowship and later on a National Science Foundation Graduate Cooperative Fellowship. Mike belongs to the IEEE and to Tau Beta Phi and Eta Kappa Nu.

Rolly Hassun

Rolly Hassun joined the -hp- Audio-Video Development Group in 1961 where he participated in the design of the -hp- Model 410C Multi-Function Voltmeter. In the Advanced Research and Development Labs, he has studied circuit noise and developed a low-noise parametric amplifier. Rolly is a graduate of the Politecnico di Milano in Italy and he earned an MSEE degree from San Jose State College. He is presently working towards the degree of Electrical Engineer at Stanford in the -hp- Honors Cooperative Program.